



Dystrophin threshold level necessary for normalisation of nNOS, iNOS and RyR1 nitrosylation in GRMD dystrophinopathy

Christel Gentil, Caroline Le Guiner, Sestina Falcone, Jean-Yves Hogrel, Cecile Peccate, Stéphanie Lorain, Sofia Benkhelifa-Ziyyat, Lydie Guigand, Marie-Françoise Montus, Laurent Servais, et al.

► To cite this version:

Christel Gentil, Caroline Le Guiner, Sestina Falcone, Jean-Yves Hogrel, Cecile Peccate, et al.. Dystrophin threshold level necessary for normalisation of nNOS, iNOS and RyR1 nitrosylation in GRMD dystrophinopathy. *Human Gene Therapy*, 2016, 27 (9), pp.712-726. 10.1089/hum.2016.041 . hal-01340106

HAL Id: hal-01340106

<https://hal.sorbonne-universite.fr/hal-01340106>

Submitted on 30 Jun 2016

HAL is a multi-disciplinary open access archive for the deposit and dissemination of scientific research documents, whether they are published or not. The documents may come from teaching and research institutions in France or abroad, or from public or private research centers.

L'archive ouverte pluridisciplinaire **HAL**, est destinée au dépôt et à la diffusion de documents scientifiques de niveau recherche, publiés ou non, émanant des établissements d'enseignement et de recherche français ou étrangers, des laboratoires publics ou privés.

Dystrophin threshold level necessary for normalisation of nNOS, iNOS and RyR1 nitrosylation in GRMD dystrophinopathy

Christel Gentil¹, Caroline Le Guiner^{2, 3}, Sestina Falcone¹, Jean-Yves Hogrel⁴, Cécile Peccate¹, Stéphanie Lorain¹, Sofia Benkhelifa-Ziyyat¹, Lydie Guigand⁵, Marie Montus³, Laurent Servais⁴, Thomas Voit^{1*} and France Piétri-Rouxel^{1#}

Affiliations:

¹Sorbonne Universités, UPMC Univ Paris 06 / Inserm / CNRS / Institut de Myologie / Centre de Recherche en Myologie (CRM), GH Pitié Salpêtrière, 105 bd de l'Hôpital, Paris 13, France

²ATLANTIC GENE THERAPIES / Inserm UMR 1089 Université de Nantes, CHU de Nantes, IRT1, 8 Quai Moncousu, BP 70721, 44007 Nantes Cedex 1, France

³GENETHON, 1 bis, rue de l'Internationale, 91000 Evry, France

⁴Institut de Myologie, GH Pitié-Salpêtrière, 75651 Paris Cedex 13, France

⁵ATLANTIC GENE THERAPIES / INRA UMR 703, Oniris, Nantes-Atlantic national college of veterinary medicine, food science and engineering, CS 44706, Nantes, F-44307, France.

*current address: NIHR Biomedical Research Centre, Institute of Child Health, University College London, 30 Guilford Street, London WC1N 1EH, UK

#Correspondence should be addressed to France Piétri-Rouxel

Sorbonne Universités, UPMC Univ Paris 06 / Inserm / CNRS / Institut de Myologie / Centre de Recherche en Myologie (CRM), GH Pitié Salpêtrière, 105 bd de l'Hôpital, Paris 13, France

france.pietri-rouxel@upmc.fr

+33 1 40 77 96 31

Short title: Threshold of dystrophin for NOS/RYR1 reinstatement

ABSTRACT

Currently, the clinically most advanced strategy to treat Duchenne muscular dystrophy (DMD) is the exon skipping strategy. Whereas antisense oligonucleotide-based clinical trials are underway for DMD, it is essential to determine a dystrophin restoration threshold needed to ensure improvement of muscle physiology at the molecular level. A preclinical trial was recently conducted in golden retriever muscular dystrophy (GRMD) dogs treated in a forelimb by locoregional delivery of rAAV8-U7snRNA to promote exon skipping on the canine dystrophin messenger. Here, we exploited the rAAV8-U7snRNA transduced GRMD muscle samples, well-characterized for their percentage of dystrophin-positive fibers, in the aim to define a threshold of dystrophin rescue necessary for normalization of the status of the neuronal nitric oxide synthase mu (nNOS μ), the inducible nitric oxide synthase (iNOS), and the ryanodine receptor-calcium release channel type 1 (RyR1), crucial actors for an efficient contractile function. Results showed that the restoration of dystrophin in 40% of muscle fibers is needed to decrease the abnormal cytosolic nNOS μ expression and to reduce the overexpression of iNOS, these two parameters leading to a reduction of the NO level into the muscle fiber. Furthermore, the same percentage of dystrophin-positive fibers of 40 % was associated with the normalization of the RyR1 nitrosylation status and to a stabilization of the RyR1/calstabin1 complex that is required to facilitate coupled gating. We concluded that a minimal threshold of 40% of dystrophin-positive fibers is necessary for the reinstatement of central proteins needed for a proper muscle contractile function, and thus identified a rate of dystrophin expression significantly improving, at the molecular level, the dystrophic muscle physiology.

INTRODUCTION

Duchenne muscular dystrophy (DMD) is a severe myopathy characterized by progressive muscle weakness with a proximal to distal course, which ultimately leads to the loss of walking ability as well as respiratory and heart failure ^{1,2}. Up to date, no curative treatment is available. The disease is caused by a null mutation in the dystrophin gene (*DMD*) and about two third of mutations cause a frameshift of the *DMD* open reading frame (ORF) inducing protein deficiency ³. In these cases, the most promising therapeutic approach is the use of antisense oligonucleotides (AOs) inducing specific exon skipping in order to restore an in-frame dystrophin mRNA and allow the production of a truncated, but still functional, protein ⁴⁻⁶. If a relative efficacy of chemically modified AOs was recently obtained in DMD patients ^{7,8}, the levels of dystrophin restoration are limited and the long-term safety and efficacy of such AOs still remain to be demonstrated. Currently, applied AO chemistries also have the drawback of limited uptake in the heart and some adverse effects, and must be administered regularly. As an alternative, rAAV-mediated delivery of small nuclear RNAs (snRNAs), especially U7snRNA, have been used to carry antisense sequences ⁹. Vectorised in recombinant adeno-associated virus (rAAV), the non-integrating snRNA-antisense constructs ensure a long term production of the therapeutic antisense sequences in X-linked muscular dystrophy mouse (mdx) and in the canine DMD model, the golden retriever muscular dystrophy (GRMD) dog ^{10,11}.

Recently, a preclinical trial has been conducted in dystrophic GRMD dogs treated in a forelimb by loco-regional delivery of rAAV8-U7snRNA inducing specific exon skipping in order to restore an in-frame dystrophin mRNA ¹². This study aimed to optimize the injection protocol, identify the safety profile and define a therapeutic dose and allowed the definition of a threshold of 40% of dystrophin expressing fibers needed to detect a significant improvement of strength ¹².

While the recovery of muscle strength is an essential parameter for quantifying the benefit of therapies, the definition of a rate of dystrophin-positive fibers capable of improving the muscle pathophysiology at the molecular level remains an important point to investigate. In the present work, we utilized the rAAV8-U7snRNA transduced GRMD muscle samples, well-characterized for their percentage of dystrophin-positive fibers, to define a threshold of dystrophin rescue necessary to

recover the status of the neuronal nitric oxide synthase mu isoform (nNOS μ), the inducible nitric oxide synthase (iNOS) and the ryanodine receptor-calcium release channel type 1 (RyR1). Indeed, it is well known that muscle function is dependent on the integrity of the dystrophin complex associated proteins, including the presence of nNOS μ . Therefore, we paid particular attention to its expression and its location. nNOS μ binds to dystrophin, via its rod domain at spectrin-like repeats 16 and 17 (R16/17)¹³. The lack of dystrophin leads, directly or indirectly, to the delocalization of nNOS μ from the sarcolemma and its accumulation in the cytosol inducing vasoconstriction and necrosis in contracting muscles¹⁴ as well as to structural defects of the neuromuscular junction¹⁵. Another isoform of NOS called iNOS is absent or present at very low level in normal skeletal muscles¹⁶, nevertheless its expression is increased in inflamed tissues^{17,18}. Interestingly, iNOS protein is up-expressed in muscles of mdx mice and DMD patients^{19,20} and its expression is reduced by gene transfer of dystrophin or utrophin in mdx mice²⁰. In dystrophic muscle, both nNOS μ mislocalization and iNOS up-regulation lead to abnormal NO production in the cytosol altering skeletal muscle contractility via the excessive S-nitrosylation of proteins, including RyR1. RyR1 contains a large number of free thiols whose nitrosylation influences channel function²¹ and its hypernitrosylation is associated with depletion of immunophilin FKBP12 (calstabin1) from the RyR1 complex²². The role of calstabin1 is to stabilize the RyR1 complex and it is required for its optimal function especially to facilitate coupled gating^{23,24}. Consequently, dissociation of calstabin1 from RyR1 complex, described in muscle of mdx mice²⁵, results in leaky calcium channels which alters the excitation-contraction coupling and thus impacting on the strength/function of the muscle.

Here, taking advantage of a preclinical study achieved in the GRMD model that provided well-characterized muscular samples displaying an increasing percentage of dystrophin-positive fibers, we defined the threshold of dystrophin expressing fibers necessary for the normalization of the status of two NOS proteins and the RyR1/calstabin1 complex, central proteins for efficient contractile function.

MATERIALS AND METHODS

Animals and study design

Dog muscle samples used in the present study were obtained from the preclinical study, designed in Atlantic Gene Therapies laboratory, which was based on the delivery of rAAV8-U7snRNA for specific exon skipping in order to restore an in-frame dystrophin mRNA¹². Dogs were part of breeding Center of Domaine des Souches (Mezilles, France) or of the Boisbonne Center for Gene Therapy (ONIRIS, Atlantic Gene Therapies, Nantes, France). The Institutional Animal Care and Use Committee of the Region des Pays de la Loire (University of Angers, France) approved all the protocol (authorization # 2011.31 obtained in 2011). The dogs were injected through locoregional transvenous injection in one forelimb with 5E+13 vg/kg of a therapeutic rAAV8-U7snRNA-E6/E8 vector, as described in Le Guiner et al.¹². The injection was done in the cephalic vein after having placed a tourniquet above the elbow of the injected forelimb. 14 weeks post injection, euthanasia was performed by intravenous injection of pentobarbital sodium (Dolethal, Vetoquinol). The samples were collected in the area located after the tourniquet, for the paws injected or not with the vector. Two untreated GRMD dogs that received the vehicle only and one wild-type (WT) dog were used as controls. Dog samples flash frozen in liquid nitrogen were used for western blot and immunoprecipitation experiments (D8, D13 and D14 dogs) and histology was carried out on sections collected from muscle samples frozen in isopentane cooled in liquid nitrogen (D8 and D13 dogs). These muscles were obtained either in the injected forelimb, either in the non-injected forelimb, as precised in Table S1.

Antibodies

For dystrophin immunolabeling, we used a rabbit polyclonal antibody (Thermo Scientific) or a goat polyclonal antibody (Santa Cruz). For nNOS, we used a rabbit polyclonal antibody (BD Biosciences) for immunolabeling and a mouse monoclonal antibody (BD Biosciences) for western blot. For iNOS detection, we used a rabbit polyclonal antibody (Abcam). We used a mouse monoclonal antibody anti-GM130 (BD Biosciences) and a rabbit polyclonal antibody anti-CD11b (Abcam) as markers of Golgi

complex and macrophages, respectively. To check nitrosylation of RyR1, both a mouse monoclonal antibody anti-RyR1 (Thermo Scientific) and a rabbit polyclonal anti-S-Nitroso-Cysteine (Cys-NO) antibody (Sigma-Aldrich) were used. For RyR1 immunoprecipitation, the mouse monoclonal antibody (Thermo Scientific) was used and for the detection by western blot, we used a polyclonal antibody anti-RyR1 (a kind gift from Dr I. Marty) and a polyclonal antibody anti-calstabin1 (Abcam). For actin, we used a mouse monoclonal antibody (Sigma-Aldrich). For Na/K ATPase, marker of membranes, we used a monoclonal antibody (GENETEX) and for GAPDHm marker of cytosol, we used a polyclonal antibody (Santa Cruz). Secondary antibodies for immunolabeling were from Life Technologies (Alexa fluor 488, 594 and 633 conjugates). For western blot, secondary antibodies coupled to horseradish peroxidase were from Jackson ImmunoResearch Laboratories, Inc and for RyR1 nitrosylation experiments, we used IRDye 680 conjugated goat anti-mouse IgG and IRDye 800CW conjugated goat anti-rabbit IgG from Li-Cor.

Histology and immunolabeling

For muscle analysis, tissue sections were cut at 8 μ m on a cryostat, fixed in 4% paraformaldehyde for 10 min and stained with hematoxylin-eosin. Images were acquired using Leica DM R microscope.

For immunolabeling, cryosections of 8 μ m were permeabilized with 0.25% Triton X-100 and blocked in PBS / 10% foetal bovine serum (FBS) for 1 h. Sections were incubated in PBS / 2% FBS with primary antibodies overnight at 4°C and washed in PBS. Sections were then incubated with secondary antibodies for 1 h, PBS washed, incubated with 4',6'-diamidino-2-phenylindole (DAPI) for nuclear staining and mounted in Fluoromount-G (Clinisciences). Images were acquired using macroscope NIKON AZ100 or Leica SPE confocal microscope.

Co-staining Dystrophin/NADPH diaphorase activity

To assess NADPH diaphorase activity, tissue sections were fixed in 4% paraformaldehyde for 8 min, permeabilized with 0.25% Triton X-100 for 10 min and then incubated with 0.2 mg / ml NBT (nitroblue tetrazolium with phosphate buffer with NaCl) and 2 mg / ml NADPH (β -nicotinamide adenine dinucleotide phosphate reduced) (Sigma-Aldrich) in PBS / 0.25% Triton X-100 for 3 h at

37°C in the darkness. Sections were then washed in PBS and treated for dystrophin immunolabeling. Sections were mounted in Fluoromount-G (Clinisciences). Images were acquired using Nikon Ti microscope.

Muscle tissue lysate

For nNOS and iNOS detection in western blot and for RyR1 protein immunoprecipitation, muscle tissues were homogenized using a dounce homogenizer in lysis buffer containing 50 mM Tris-HCl, pH 7.4, 100 mM NaCl and 0.5% NP-40 with a mix of protease inhibitors. For RyR1 nitrosylation experiments, tissues were homogenized in lysis buffer containing 200 mM sucrose, 20 mM HEPES pH 7.4 and 0.5 mM CaCl₂ with a mix of protease inhibitors.

Membranes and cytosol fractionation

We performed membrane-cytosol fractionation using Mem-PER™ Plus Membrane Protein Extraction Kit (Thermo Scientific). Total lysate, membrane fraction and cytoplasmic fraction were isolated from 35 mg of muscle, following manufacturer instructions for hard tissues. 40 µg of total and membrane proteins and 60 µg of cytoplasmic proteins were used for western blotting. Quantification was performed using Quantity one software.

Immunoprecipitation

Samples were centrifuged for 10 min at 14000 g and 600 µg of proteins were precleared with 20 µl washed protein G-Sepharose (PGS 4 fast flow; GE Healthcare) then incubated with mouse monoclonal anti-RyR1 antibody or with mouse anti-IgG overnight at 4°C. Then, 40 µl of protein G-Sepharose beads were added for 2 h at 4°C. Beads were collected by centrifugation and washed with lysis buffer. Proteins were eluted in Laemmli buffer.

Western blotting

For nNOS and iNOS detection and for RyR1 protein immunoprecipitation, samples were centrifuged for 10 min at 14000 g and denatured at room temperature for 30 min with Laemmli buffer. For RyR1 nitrosylation experiments, samples were centrifuged for 5 min at 1500 g and remained in non-

denaturing and non-reducing conditions. Proteins were separated by electrophoresis (NuPage 4-12% Bis-Tris Gel ; Life Technologies), then transferred to nitrocellulose membranes and labeled with primary antibodies and secondary antibodies coupled to horseradish peroxidase or IRDye secondary antibodies for the Odyssey Infrared System (Lycor). Quantification was performed using Quantity one software.

Functional assessment

The functional assessment was performed during the pre-clinical study conducted by Le Guiner's team¹². Briefly, movements of flexion and extension of the carpal joint were elicited by subcutaneous stimulation of the common branch of the medial and ulnar nerves for flexion measurements or of the radial nerve for extension measurements. Stimulations were performed at seven different frequencies from 5 to 200 Hz. Signals were analysed at the end of the experiment and the maximum value obtained at each stimulation frequency was recorded to obtain the frequency response curve for each function tested. Values were obtained in volts and converted to torque (in Nm). The maximal strength value obtained over all stimulation frequencies was then expressed in percentage of predicted normal values. Three measurement sessions were planned: before injection, 1.5 months and 3 months after injection. The strength changes were expressed as a percentage of change per month.

RESULTS

Description of muscular samples used in the study

To assess the percentage of dystrophin-positive fibers that are required for the improvement of muscle physiology at the molecular level, we used dog muscle samples obtained from a preclinical trial based on the delivery of rAAV8-U7snRNA for specific exon skipping in order to restore an in-frame dystrophin mRNA¹²; more details on this study are reported in "Methods" section. Because we were especially interested in selecting muscle samples with increasing amount of dystrophin-positive fibers, we took advantage of collecting muscle samples previously well characterized for their percentage of dystrophin-positive fibers. Indeed, as reported in study Le Guiner et al., the percentage of dystrophin positive fibers were quantified after immuno-peroxidase staining of frozen transverse sections of the

muscles using a specific anti-dystrophin antibody (NCL-DYS2), by manual count. For each section, a total of at least 250 fibers were counted¹². A fiber was considered positive when more than third of its circumference exhibited a staining more intense than negative controls (negative fibers in untreated GRMD dogs).

Based on these data, we classified the collected muscle samples in four groups, depending on the percentage of dystrophin-positive fibers on each muscle section as follows: the percentage of dystrophin-positive fibers is less than 20% (<20%); between 20 and 30% (20-30%); between 40 and 50% (40-50%); or over 65% (>65%) (Table S1). One wild-type (WT) dog, two untreated GRMD dogs (dogs C1 and C2) and three treated GRMD dogs (dogs D8, D13 and D14) were included for molecular investigations. To validate the dystrophin expression in all the muscle samples used in the present study, immunofluorescent labeling analyses were performed (Figure 1A).

Positive dystrophin fibers were counted on sections of muscle taking into account that in muscle sections of GRMD dogs a diffuse labeling within necrotic fibers was a non-specific staining. The estimating amount of dystrophin-positive fibers was in a good accordance with the dystrophin quantification performed in the study of Le Guiner et al.¹². Furthermore, to confirm that the dystrophin-positive fibers detected on sections were positive all along the fiber reflecting thus the percentage of positive fibers to the entire muscle, we performed immunostaining for dystrophin on sections displaying longitudinal fibers. Analysis of dystrophin labeling on these sections confirmed that a fiber was dystrophin-positive or dystrophin-negative along its entire lengths (Figure 1B). To investigate histopathophysiological features of muscles, hematoxylin and eosin staining was performed on sample cryosections (Figure 1C). In muscles from the WT dog, fibers were uniform in both size and shape and nuclei were peripherally localized. GRMD muscles presented typical dystrophic features including heterogeneity in fiber size, few centralized nuclei, infiltrating mononuclear cells, endomysial fibrosis and adiposis. In accordance with Le Guiner et al.¹², an histological improvement with more uniform fibers, less fibrosis and adipose tissue was observed in muscle samples presenting more than 40% of dystrophin-positive fibers.

Determination of percentage of dystrophin-positive fibers needed for proper localization and expression of nNOS μ protein

To investigate the nNOS μ protein expression in the different canine muscle samples, western blotting was achieved on total protein extracts from the four classes of muscle samples (<20%, 20-30%, 40-50%, and >65%) (Figure 2A). Results showed a 160 kDa band corresponding to the muscular nNOS μ isoform and the quantification of band intensity revealed equal level in WT, untreated and treated GRMD dogs whatever the percentage of dystrophin-positive fibers. To answer to the question of what percentage of dystrophin-positive fibers is needed for recovering proper nNOS μ localization, immunolabeling of dystrophin and nNOS μ was investigated in the four classes of muscle samples (Figure 2B). Immunolabeling carried out on sections of WT dog muscle confirmed nNOS μ co-localization with dystrophin at the sarcolemma. In untreated GRMD muscles, nNOS μ was detected into the cytosol as aggregates with an accumulation under the sarcolemma and in the perinuclear zone. To support imaging results, subcellular fractionation experiments were performed with muscle samples from control, GRMD and treated muscle expressing >65% of dystrophin positive fibers. Data showed the presence of nNOS μ protein in the cytosol fraction obtained from GRMD muscle samples while no protein could be detected in the cytosolic fractions performed from control nor from GRMD dog expressing more than 65% of dystrophin positive fibers. Furthermore, nNOS μ protein was found in the enriched membrane fractions from control and treated GRMD >65% muscle samples while a weak band was observed for the non-treated GRMD muscle sample (Figure S2).

To precise the cytosolic nNOS μ location, we achieved a double immunofluorescent labeling of this compartment and nNOS μ protein using GM130, a marker of Golgi apparatus, and nNOS μ antibodies respectively (Figure 2B). In WT muscles, Golgi puncta were localized principally around the nuclei while a few were localized deeper inside the fiber. In untreated GRMD muscles, the Golgi apparatus was disorganized and accumulated in the cytosol. Cytosolic nNOS μ was not colocalized with Golgi puncta but appeared near the Golgi apparatus as aggresome-like inclusions as already described in primary cortical neurons²⁶.

In muscle samples displaying less than 30% of dystrophin-positive fibers, the nNOS μ was detected in cytosol and in sub-sarcolemmal aggregates. Surprisingly, this abnormal location was observed in both dystrophin negative and positive fibers. Nevertheless, a partial sarcolemmal location of nNOS μ was

observed in few fibers exhibiting a strong positive dystrophin staining and a correct organization of the Golgi complex. In treated muscles presenting more than 40% of dystrophin-positive fibers, a major reduction of nNOS μ staining in the cytosol and the sub-sarcolemmal region was detected. Additionally, while proper location of nNOS μ to the sarcolemma required the presence of the dystrophin at the membrane, unexpectedly, the disappearance of cytosolic nNOS μ staining was observed in both positive and negative fibers for dystrophin. Similarly, in these muscle samples, the Golgi apparatus organization was restored in all fibers.

Determination of percentage of dystrophin-positive fibers needed for a proper expression of iNOS protein

Untreated GRMD muscle sections stained with hematoxylin and eosin revealed the presence of strong cellular infiltrates (Figure 1C) confirmed by the immunolabeling of CD11b-positive macrophages (Figure S3). This prompted us to focus on the expression of iNOS, which has been described to be up-regulated in inflamed tissues and thus strongly expressed in dystrophic muscles²⁰. To evaluate its expression in the GRMD dog model, a western blot analysis was performed on total protein extracts from the different muscle samples (Figure 3A). Results showed that untreated GRMD muscles displayed an eight-fold increase of iNOS protein expression compared with WT muscles and that under 30% of dystrophin-positive fibers, treated muscles presented an eight-fold increase of iNOS expression, similar to untreated GRMD muscles. The restoration of dystrophin in over 40% of fibers resulted in a significant halving of iNOS expression in the muscle extracts.

These findings were confirmed by immunolabeling experiment (Figure 3B) showing, as expected, a strong iNOS expression in infiltrating cells, but also an up-expression into the cytosol and at the sarcolemma of all muscle fibers of the GRMD muscles. This is in stark contrast to WT muscles where iNOS was only detectable in interstitial cells. These data confirmed that iNOS expression was associated with infiltration by inflammatory cells and was up-expressed in untreated GRMD muscle fibers. Furthermore, the data showed that in muscle samples containing less than 20% of dystrophin-positive fibers, iNOS was highly expressed into fibers and in interstitial cells as observed in untreated GRMD dogs (Figure 3B). In muscle sections displaying between 20-30% of dystrophin-positive fibers, iNOS expression detected by western blot was not significantly different compared to the

GRMD muscle samples (Figure 3B), however immunofluorescence experiment allowed discriminating the iNOS protein location, decreasing into the fibers while an intense labeling remained obvious between the interstitial cells (Figure 3B). When more than 40% of fibers were positive for dystrophin, the rescue of dystrophin was correlated with a reduction of iNOS expression in the whole muscle.

Determination of percentage of dystrophin-positive fibers for a proper NOS enzymatic activity

To correlate the NOS protein expression and location to their enzymatic activity, we achieved the detection of the NADPH-diaphorase activity as a marker for nitric oxide synthase²⁷ by colorimetric staining concomitantly to the detection of dystrophin by immunofluorescence (Figure 4). As expected, the labelling of NO production in the fibers was strictly sarcolemmal in WT muscles certainly due to the nNOS μ presence at the membrane. On the contrary, in GRMD muscle fibers, NO accumulation was found into the cytosol, in the sub-sarcolemma region and in interstitial areas, results which were well correlated with what was observed for the nNOS μ and the iNOS expression and location. In muscle samples displaying less than 30% of dystrophin-positive fibers, NO was found accumulate in the cytosol and in sub-sarcolemma region in both dystrophin negative and positive fibers. In treated muscles expressing more than 40% of dystrophin-positive fibers, NOS enzymatic activity was detected at the sarcolemma in dystrophin-positive fibers associated with a major reduction of cytosolic NO production. This decrease was even observed in some negative-dystrophin fibers. When more than 65% of fibers were positive for dystrophin, NADPH-diaphorase staining was similar to that observed in WT muscles. In accordance with the above data, these results revealed that a restoration of dystrophin in 40% of muscle fibers was needed to lead to a reduction of the NO level within the fibers.

Determination of percentage of dystrophin-positive fibers needed to normalize RyR1-calstabin1 complex status

Cytosolic NO produced by cytoplasmic nNOS μ and iNOS could alter skeletal muscle contractility via the S-nitrosylation of RyR1 and could subsequently reduce the affinity of calstabin1 for RyR1^{21,22}. In this regard, RyR1 expression and its nitrosylation state were investigated by a multiplex western blotting on muscle sample lysates from untreated and treated GRMD muscles and compared to WT

muscles (Figure 5A). While the total RyR1 levels were identical in untreated GRMD and WT muscle extracts, S-nitrosylation of the RyR1 cystein residues was detected only in untreated GRMD muscles. The data revealed that the expression levels of RyR1 were lower in treated GRMD muscles than in WT and untreated GRMD muscles; this difference is probably due to the sensitivity of the RyR1 protein to the sample storage conditions. The nitrosylation status of the RyR1 was investigated in the four classes of treated GRMD muscle samples and showed that RyR1 was hypernitrosylated, in muscle samples presenting a level below 30% of dystrophin-positive fibers as observed in untreated GRMD samples. Interestingly, S-nitrosylation of RyR1 decreased when muscles expressed more than 40% of dystrophin-positive fibers and was almost undetectable in muscles displayed more than 65% of dystrophin-positive fibers. These data were confirmed by confocal microscopy analysis of S-nitrosocysteine (Cys-NO) expression achieved on muscle sections of untreated and treated GRMD muscles compared to WT muscles (Figure 5B). Indeed, a higher Cys-NO expression level was observed in untreated GRMD muscles in comparison to WT muscles. In accordance with western blotting, the level of the nitrosylated RyR1 was inversely proportional to the level of dystrophin rescue in muscles from treated GRMD dogs. These data demonstrated that minimal percentage of 40% to 65% of dystrophin-positive fibers were needed to return to the physiological RyR1 state.

To study the impact of RyR1 hypernitrosylation on the calstabin1-RyR1 interaction, RyR1 was immunoprecipitated (IP RyR1) from muscle samples of WT, untreated and treated GRMD dogs (Figure 5C). Both total and immunoprecipitated proteins were immunoblotted with antibodies against RyR1 and calstabin1. Inputs confirmed that the total amount of RyR1 and calstabin1 were identical in all muscle extracts. A twenty-fold decrease of the calstabin1 bound to the RyR1, compared to WT muscle extracts, was observed in non-treated GRMD muscles and when the number of dystrophin-positive fibers was inferior to 20%. However, more than 40% of dystrophin-positive fibers was associated to a stabilized calstabin1-RyR1 interaction with a significant six-fold enhancement of calstabin1 binding to RyR1. Overall, these data revealed that restoration of dystrophin in at least 40% of muscle fibers allowed an increased RyR1 channel stability and suggested an improvement of the excitation contraction coupling.

To establish a link between these molecular data and muscular function, RyR1 nitrosylation status was investigated precisely in untreated or treated *flexor carpi ulnaris* muscles and *extensor carpi radialis* muscles previously used for measurement of force generation in the three treated GRMD dogs (D8, D13 and D14 dogs) included in the preclinical previous study¹². We collected data of force measurements and the corresponding muscle samples for S-nitrosylation of the RyR1 status investigation for two (D8 and D14 dogs) of these three dogs. Flexion and extension strengths were evaluated at the wrist using a custom-made torque measurement device (Figure 5D). Three measurements were carried out to define a strength change along the protocol: before injection, 1.5 months post-injection and 3 months post-injection. In muscles from non-injected control forelimb, the percentage of dystrophin-positive fibers may be 20%, due to diffusion of the therapeutic vector in the contralateral limbs, whereas the treated muscles displayed at least 65% of dystrophin-positive fibers. As described in Le Guiner et al.¹², treated muscles exhibiting more than 65% of dystrophin-positive fibers, displayed an increase of strength between 4,7% and 18,3% for *flexor* and between 9,5% and 11% for *extensor* muscles compared to non-injected contralateral muscles. RyR1 nitrosylation status was then precisely investigated in both in *flexor* and *extensor* (from the D8 and D14 dogs) expressing (i) less than 20% or (ii) more than 65% of dystrophin-positive fibers and compared to muscles from WT and untreated GRMD dogs (Figure 5E). The profile of RyR1 expression observed in the multiplex western blotting was slightly different between the two treated GRMD dogs (D8 and D14), this difference was probably due to the sensitivity of the RyR1 protein to the conditions of sample storage. Nevertheless, the muscles that expressed less than 20% of dystrophin-positive fibers exhibited an increased S-nitrosylation of RyR1 which was almost undetectable when muscles presented more than 65% of dystrophin-positive fibers. These data strongly suggested RyR1 status normalization observed in treated GRMD muscles was correlated with an improvement of muscle strength.

DISCUSSION

The present study outlined, for the first time in the dystrophic GRMD dog model, that restoration of dystrophin in 40% of muscle fibers is needed for reinstatement of molecular actors reported to be essential for assuring an efficient contractile function and for improving the global physiopathology state of the treated muscle.

Previous investigations to determine dystrophin levels required to improve muscle function have already been performed in the mdx mouse model by using phosphorodiamidate morpholino oligomer (PMO) to modulate dystrophin pre-mRNA by exon skipping^{28,29}. These studies concluded that 15-20% of dystrophin expression were sufficient to protect dystrophic muscle against exercise-induced damage but were not enough to enhance muscle strength. However, a series of repeated injections for 20 weeks allowed an increase in specific isometric force correlated with an average of 50% dystrophin-positive fibers in the *tibialis anterior* muscles. It is well known that mdx muscles are less affected by the absence of dystrophin compared to the GRMD muscles which display a more severe phenotype mimicking the progressive degeneration observed in human DMD muscles resulting for the GRMD dogs in an important reduction of life span³⁰. The differences between the species could account for the variable thresholds of dystrophin levels needed to obtain physiological benefits. Indeed, in the GRMD dog model, two studies have described benefits of dystrophin rescue with exon skipping strategy in skeletal muscles from GRMD dogs^{11,12}. The first showed that intramuscular injection of 3-week-old GRMD puppies allowed a dystrophin rescue of about 80%, however, this protocol was not designed to define a dystrophin threshold level to improve the muscular contractile function. Secondly, dogs at 3-4 months of age were injected by locoregional transvenous perfusion with different therapeutic doses and showed a significant decrease of myofiber regeneration, endomysial and total fibrosis when the percentage of dystrophin-positive fibers was at least 33%. Nevertheless, the strength increase was observed when muscles displayed a restoration of dystrophin of at least 40% of fibers. Finally, regarding the correlation between the levels of dystrophin-positive fibers and muscle force, 40 to 50 % of dystrophin-positive fibers are required to observe an improvement of muscle strength whatever the studies and the animal models.

Today, there is a growing interest to restore dystrophin in DMD patients, while the major evaluation of the therapeutic benefice is the measurement of the improvement of muscle strength, increasing need

remains for determining the levels of dystrophin restoration that are required for improving the muscle pathophysiology at the molecular levels. Here, in an attempt to answer this question, we focused the assessments on the status of two NOS proteins and the RyR1/calstabin1 complex because of their crucial roles for assuring the efficiency of contractile function.

Dystrophin rescue leads to proper NOS protein expression and location

In DMD, the lack of dystrophin leads to nNOS mislocalization from the sarcolemma to the cytosol causing a functional ischemia and an exacerbating fatigue response to exercise^{14,31}. nNOS μ is then accumulated in the cytosol inducing nitrosative stress and impaired muscle contraction³². In mdx mice, restoration of dystrophin expression by gene therapy allowed the recovery of nNOS μ at the sarcolemma which was associated with physiological benefits^{33–35}. In our previous study involving muscle samples from BMD patients carrying spontaneous 45–55 deletion in the *DMD* gene affecting the nNOS μ -binding domain, we correlated the severity of the dystrophic phenotype with the degree of cytosolic nNOS μ localization³⁶. In this study, the proper relocation of the sarcolemma nNOS μ was systematically observed as concomitant to the rescue of dystrophin expression. In addition, the situation of abnormal cytosolic nNOS μ observed in untreated GRMD was totally absent in the muscles having 40% of dystrophin-positive fibers, and this in the entire muscle comprising both, positive and negative dystrophin fibers. This observation was consistent with what was observed when the activity of NADPH was measured concurrently with the dystrophin expression (Figure 4) where in some fibers the NADPH activity was very low although dystrophin was not expressed. Moreover, analysis of histopathophysiological features of this class of muscle expressing 40% of dystrophin positive fibers revealed a remarkable improvement of the phenotype suggesting that it is more linked to the decrease of cytosolic nNOS than to the proper sarcolemmal localization.

The dystrophin expression and the loss of cytosolic nNOS μ in treated muscles were correlated with a restoration of normal Golgi apparatus organization. Previous studies have suggested that the cytosolic nNOS protein could correspond to the nNOS β isoform, a nNOS splice variant. This isoform was first described being localized at the Golgi complex in mdx skeletal muscle and suggested to be involved in compensation mechanisms such as hypertrophy³⁷. In GRMD dogs, we showed that cytosolic nNOS

seems to form aggresome-like inclusions localized adjacent to Golgi cisternae as previously observed in primary cortical neurons²⁶ but was not colocalized with the Golgi complex. Moreover, we were not able to detect the presence of nNOS β isoform described to be associated to the Golgi, either by RT-PCR or with a specific antibody suggesting that this isoform does not correspond to the cytosolic nNOS that was observed in the GRMD muscles.

The other member of the NOS protein family studied here, iNOS, was found to be overexpressed in dystrophic muscles displaying a strong inflammation. In mdx mice, dystrophin expression or utrophin overexpression by gene transfer reduce the iNOS expression²⁰. Our findings also demonstrated that iNOS expression was inversely correlated to the dystrophin expression level and allowed defining a percentage of 40% of dystrophin-positive fibers that totally suppresses its expression in interstitial cells and into myofibers. Nevertheless, contribution of iNOS in the pathophysiology of DMD remains unclear. Two teams have independently generated iNOS/dystrophin-double null mice and could not observe changes in macrophage infiltration^{38,39}. However, while Villalta et al. showed that ablation of iNOS in mdx mice reduced muscle fiber injury of the *soleus* muscle, Li et al. found that the removal of iNOS in mdx did not improve muscle histopathology and specific force of the *extensor digitorum longus* muscle. A possible explanation for such contradictory results could be linked to the different fiber type compositions (fast or slow twitch) of the muscles studied or to a different muscle solicitation.

Dystrophin rescue leads to normalization of RyR1-calstabin1 complex status correlated with an improvement of strength

Previous studies have attempted to define the NOS, iNOS or nNOS μ , responsible for nitrosylation of RyR1. Bellinger et al. suggested that S-nitrosylation of RyR1 has to be attributed to iNOS activity in mdx mouse on the basis that iNOS protein was immunoprecipitated with RyR1 and that nNOS μ expression was decreased in mdx muscle²⁵. However, Salanova et al. showed a co-localization of RyR1 and nNOS μ in myofibers from normal human skeletal muscle⁴⁰ and Li et al. showed that the absence of nNOS μ in dystrophin/nNOS μ double-deficient mice minimized RyR1 S-nitrosylation improving muscle force³². While this question remains open for the time being, our study showed that

total nNOS μ was not reduced in GRMD muscle and that both NOS proteins disappeared concomitantly from the muscle cytosol following dystrophin rescue leading to RyR1 status normalization.

Our findings show, for the first time, that dystrophin rescue in over 40% of the muscle fibers corrected the RyR1 nitrosylation status which was correlated with the return of the calstabin1-RyR1 complex stability. However, several studies showed that a default in RyR1 channel activity due to the dissociation of calstabin1, led to defective calcium signaling and impaired skeletal muscle contractility^{23,24}. Restoration of calstabin1 binding to RyR1 then appears as an interesting therapeutic strategy. In this context, drugs such as S107, which prevents the depletion of calstabin1 from the RyR1 complex, have been developed. In mdx mice, RyR1 status normalization using S107 was correlated with an improvement of grip strength²⁵. In the dog model, force measurement protocols are not suitable to measure the force generated by a specific muscle. One protocol has been developed to record strength in a single intact muscle in dystrophin-deficient dogs⁴¹ but it was not appropriate to our study because this procedure required an important surgical device and animals must be euthanized at the end of the experiment. In the present study, the protocol allowed attribution of the force generated mostly to one specific *flexor* and one specific *extensor* muscle. Coherently with our hypothesis, we observed RyR1 status normalization in these treated GRMD muscles resulted in an improvement of strength.

A threshold of 40% of dystrophin-positive fibers is necessary to improve molecular parameters crucial for efficient contractile function

The present study raises the provocative question which asks if the dystrophin is the major provider of the global beneficial effect observed in the muscle as a whole. Indeed, in these conditions where 60% of the fibers do not express dystrophin, the muscle should remain susceptible to mechanical trauma with subsequent muscle fiber loss in an inflammatory environment. However, in the muscles having 40% of dystrophin-positive fibers or more, abnormal cytosolic nNOS μ was totally absent and NADPH activity was low and this in whole the muscle. In regards to iNOS expression, the iNOS level in dystrophin-positive fibers versus dystrophin-negative fibers were quantified by counting on muscle sections co-labelled for dystrophin and iNOS (Figure S4). This quantification confirmed that, even if

the iNOS staining significantly decreased in muscle samples presenting more than 40% of positive fibers, the iNOS level in dystrophin-positive fibers versus dystrophin-negative fibers was not significantly different. We assume thus that the improvement of the muscle dystrophic status should not be attributed restrictively to the local mechanical and structural role of dystrophin as being the single determinant of muscle fiber health. This question has already discussed in comment to the study of Le Guiner et al ⁴². A more general mechanism would take place such as the decrease of the inflammatory status and in particular the reduction of the amount of macrophages leading to a decrease of the level of iNOS activation in all muscle fibers as it was observed in the present study. Moreover, a more diffuse mechanism has to be considered, the regulation of calcium homeostasis that would play a critical role in muscle fiber integrity. Indeed, it is known that high intracellular calcium concentration activates iNOS protein expression via cell lysis and macrophage activation ^{18,43} and nNOS via the calcium-calmodulin kinase activation ⁴⁴. Finally, at the molecular level, NOS protein expression and location, the RyR1 channel stabilization, and the improvement of muscle strength, are all parameters correlated to the intracellular calcium level which therefore would be a significant contributor to the general beneficial effect observed in the treated muscle even though more than half of fibers do not express dystrophin.

To conclude, the present study defines a threshold of 40% of dystrophin-positive fibers necessary for improving status of crucial proteins for efficient contractile function. The results also highlight the important point that dystrophin rescue is probably not the unique determining element for reinstating physiological status of the treated muscle, bringing thus new information for the development of successful therapeutic approach for DMD.

ACKNOWLEDGMENTS

The authors thank Pr JC. Kaplan, Dr S. Vassilopoulos and Dr Y. Chérel for their valuable contributions and Dr B. Cadot for his help in microscopy image acquisition. We thank M. Jorre, Dr C. Falcone and M. Dutilleul for their technical assistance and Dr I. Marty for kindly providing RyR1 antibody.

This work was supported by the Association Française contre les Myopathies (AFM); Association Institut de Myologie (AIM); the Centre National de la Recherche Scientifique (CNRS), the Institut National de la Santé et de la Recherche Médicale (INSERM) and Université Pierre et Marie-Curie Paris 6 (UPMC).

AUTHOR DISCLOSURE STATEMENT

Competing Interests

No competing financial interests exist.

REFERENCES

1. Hoffman EP, Brown RH and Kunkel LM. Dystrophin: the protein product of the Duchenne muscular dystrophy locus. *Cell* 1987;51:919–28.
2. Moser H. Duchenne muscular dystrophy: pathogenetic aspects and genetic prevention. *Hum Genet* 1984;66:17–40.
3. Leturcq F, Yaou RB, Hamroun D, et al. Genotype-phenotype analysis in 2,405 patients with a dystrophinopathy using the UMD-DMD database: a model of nationwide knowledgebase. *Hum Mutat* 2009;30:934–945.
4. Cirak S, Arechavala-Gomez V, Guglieri, et al. Exon skipping and dystrophin restoration in patients with Duchenne muscular dystrophy after systemic phosphorodiamidate morpholino oligomer treatment: an open-label, phase 2, dose-escalation study. *Lancet* 2011;378:595–605.
5. Dunkley MG, Manoharan M, Villiet P, et al. Modification of splicing in the dystrophin gene in cultured Mdx muscle cells by antisense oligoribonucleotides. *Hum Mol Genet* 1998;7:1083–1090.
6. Rodino-Klapac LR, Mendell JR and Sahenk Z. Update on the treatment of Duchenne muscular dystrophy. *Curr Neurol Neurosci Rep* 2013;13:332.
7. Mendell JR, Rodino-Klapac LR, Sahenk Z, et al. Eteplirsen for the treatment of Duchenne muscular dystrophy. *Ann Neurol* 2013;74:637–647.
8. Voit T, Topaloglu H, Straub V, et al. Safety and efficacy of drisapersen for the treatment of Duchenne muscular dystrophy (DEMAND II): an exploratory, randomised, placebo-controlled phase 2 study. *Lancet Neurol* 2014;13:987–996.

9. De Angelis FG, Sthandier O, Berarducci B, et al. Chimeric snRNA molecules carrying antisense sequences against the splice junctions of exon 51 of the dystrophin pre-mRNA induce exon skipping and restoration of a dystrophin synthesis in Delta 48-50 DMD cells. *Proc Natl Acad Sci U S A* 2002;99:9456–61.
10. Goyenvallé A, Vulin A, Fougère F, et al. Rescue of dystrophic muscle through U7 snRNA-mediated exon skipping. *Science* 2004;306:1796–1799.
11. Vulin A, Barthélémy I, Goyenvallé A, et al. Muscle function recovery in golden retriever muscular dystrophy after AAV1-U7 exon skipping. *Mol Ther* 2012;20:2120–2133.
12. Le Guiner C, Montus M, Servais L et al. Forelimb treatment in a large cohort of dystrophic dogs supports delivery of a recombinant AAV for exon skipping in Duchenne patients. *Mol Ther* 2014;22:1923–1935.
13. Lai Y, Thomas GD, Yue Y et al. Dystrophins carrying spectrin-like repeats 16 and 17 anchor nNOS to the sarcolemma and enhance exercise performance in a mouse model of muscular dystrophy. *J Clin Invest* 2009;119:624–635.
14. Kobayashi YM, Rader EP, Crawford RW et al. Sarcolemma-localized nNOS is required to maintain activity after mild exercise. *Nature* 2008;456:511–515.
15. Shiao T, Fond A, Deng B, et al. Defects in neuromuscular junction structure in dystrophic muscle are corrected by expression of a NOS transgene in dystrophin-deficient muscles, but not in muscles lacking alpha- and beta1-syntrophins. *Hum Mol Genet* 2004;13:1873–1884.
16. Thompson M, Becker L, Bryant D et al. (1996). Expression of the inducible nitric oxide synthase gene in diaphragm and skeletal muscle. *J Appl Physiol Bethesda Md* 1985 1996;81:2415–20.
17. Adams V, Nehrhoff B, Späte U et al. Induction of iNOS expression in skeletal muscle by IL-1 β and NF κ B activation: an in vitro and in vivo study. *Cardiovasc Res* 2002;54:95–104.
18. Altamirano F, López JR, Henríquez C et al. Increased Resting Intracellular Calcium Modulates NF- κ B-dependent Inducible Nitric-oxide Synthase Gene Expression in Dystrophic mdx Skeletal Myotubes. *J Biol Chem* 2012;287:20876–87.
19. Bia BL, Cassidy PJ, Young ME et al. Decreased myocardial nNOS, increased iNOS and abnormal ECGs in mouse models of Duchenne muscular dystrophy. *J Mol Cell Cardiol* 1999;31:1857–62.
20. Louboutin JP, Rouger K, Tinsley JM et al. iNOS expression in dystrophinopathies can be reduced by somatic gene transfer of dystrophin or utrophin. *Mol Med Camb Mass* 2001;7:355–64.
21. Sun J, Xin C, Eu JP et al. Cysteine-3635 is responsible for skeletal muscle ryanodine receptor modulation by NO. *Proc Natl Acad Sci U S A* 2001;98:11158–62.
22. Aracena P, Tang W, Hamilton SL et al. Effects of S-glutathionylation and S-nitrosylation on calmodulin binding to triads and FKBP12 binding to type 1 calcium release channels. *Antioxid Redox Signal* 2005;7:870–81.
23. Avila G, Lee EH, Perez CF et al. FKBP12 binding to RyR1 modulates excitation-contraction coupling in mouse skeletal myotubes. *J Biol Chem* 2003;278:22600–8.

24. Tang W, Ingalls CP, Durham WJ et al. Altered excitation-contraction coupling with skeletal muscle specific FKBP12 deficiency. *FASEB J Off Publ Fed Am Soc Exp Biol* 2004;18:1597–9.
25. Bellinger AM, Reiken S, Carlson C et al. Hypernitrosylated ryanodine receptor calcium release channels are leaky in dystrophic muscle. *Nat Med* 2009;15:325–30.
26. Corso-Díaz X and Krukoff TL. nNOS alpha and nNOS beta localization to aggresome-like inclusions is dependent on HSP90 activity. *J Neurochem* 2010;114:864–72.
27. Shimosegawa T and Toyota T. NADPH-diaphorase activity as a marker for nitric oxide synthase in neurons of the guinea pig respiratory tract. *Am J Respir Crit Care Med*. 1994;150:1402–1410.
28. Godfrey C, Muses S, McClorey G et al. How much dystrophin is enough: the physiological consequences of different levels of dystrophin in the mdx mouse. *Hum Mol Genet* 2015;24:4225–4237.
29. Sharp PS, Bye-a -Jee H and Wells DJ. Physiological Characterization of Muscle Strength With Variable Levels of Dystrophin Restoration in mdx Mice Following Local Antisense Therapy. *Mol Ther* 2011;19:165–71.
30. McGreevy JW, Hakim CH, McIntosh MA et al. Animal models of Duchenne muscular dystrophy: from basic mechanisms to gene therapy. *Dis Model Mech* 2015;8:195–213.
31. Sander M, Chavoshan B, Harris SA et al. Functional muscle ischemia in neuronal nitric oxide synthase-deficient skeletal muscle of children with Duchenne muscular dystrophy. *Proc Natl Acad Sci U S A* 2000;97:13818–23.
32. Li D, Yue Y, Lai Y et al. Nitrosative stress elicited by nNOS μ delocalization inhibits muscle force in dystrophin-null mice. *J Pathol* 2011;223:88–98.
33. Decrouy A, Renaud JM, Lunde JA et al. Mini- and full-length dystrophin gene transfer induces the recovery of nitric oxide synthase at the sarcolemma of mdx4cv skeletal muscle fibers. *Gene Ther* 1998;5:59–64.
34. Wells KE, Torelli S, Lu Q et al. Relocalization of neuronal nitric oxide synthase (nNOS) as a marker for complete restoration of the dystrophin associated protein complex in skeletal muscle. *Neuromuscul Disord NMD* 2003;13:21–31.
35. Zhang Y and Duan D. Novel mini-dystrophin gene dual adeno-associated virus vectors restore neuronal nitric oxide synthase expression at the sarcolemma. *Hum Gene Ther* 2012;23:98–103.
36. Gentil C, Leturcq F, Ben Yaou R et al. Variable phenotype of del45-55 Becker patients correlated with nNOS μ mislocalization and RYR1 hypernitrosylation. *Hum Mol Genet* 2012;21:3449–60.
37. Froehner SC, Reed SM, Anderson KN et al. Loss of nNOS inhibits compensatory muscle hypertrophy and exacerbates inflammation and eccentric contraction-induced damage in mdx mice. *Hum Mol Genet* 2015;24:492–505.
38. Li D, Shin J-H and Duan D. iNOS Ablation Does Not Improve Specific Force of the Extensor Digitorum Longus Muscle in Dystrophin-Deficient mdx4cv Mice. *PLoS ONE* 2011;6:e21618.

39. Villalta SA, Nguyen HX, Deng B et al. Shifts in macrophage phenotypes and macrophage competition for arginine metabolism affect the severity of muscle pathology in muscular dystrophy. *Hum Mol Genet* 2009;18:482–96.
40. Salanova M, Schiffel G, Rittweger J et al. Ryanodine receptor type-1 (RyR1) expression and protein S-nitrosylation pattern in human soleus myofibres following bed rest and exercise countermeasure. *Histochem Cell Biol* 2008;130:105–18.
41. Yang HT, Shin J-H, Hakim CH et al. Dystrophin Deficiency Compromises Force Production of the Extensor Carpi Ulnaris Muscle in the Canine Model of Duchenne Muscular Dystrophy. *PLoS ONE* 2012;7.
42. Partridge T. Could exon skipping help dystrophic boys to run, hop, and jump? *Mol Ther* 2014;22:1884–6.
43. Denlinger LC, Fiset PL, Garis KA et al. Regulation of Inducible Nitric Oxide Synthase Expression by Macrophage Purinoreceptors and Calcium. *J Biol Chem* 1996;271:337–42.
44. Weissman BA, Jones CL, Liu Q et al. Activation and inactivation of neuronal nitric oxide synthase: characterization of Ca²⁺-dependent [125I]Calmodulin binding. *Eur J Pharmacol* 2002;435:9–18.

Figure Legends

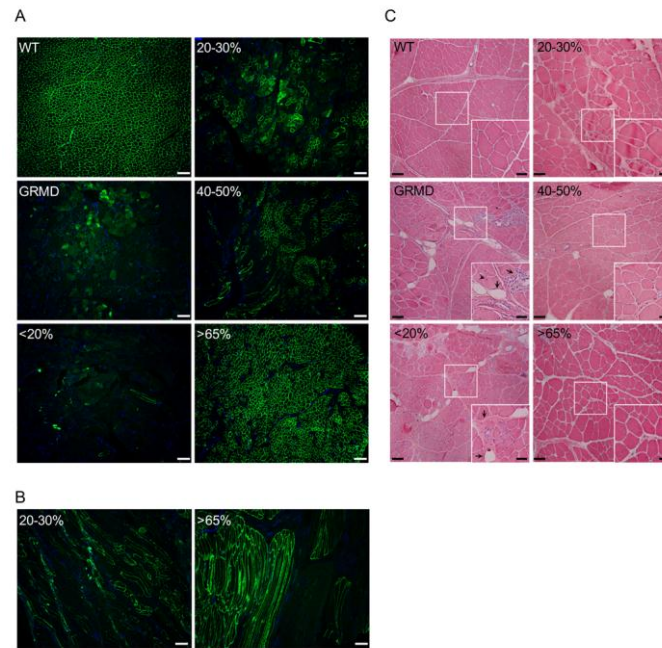


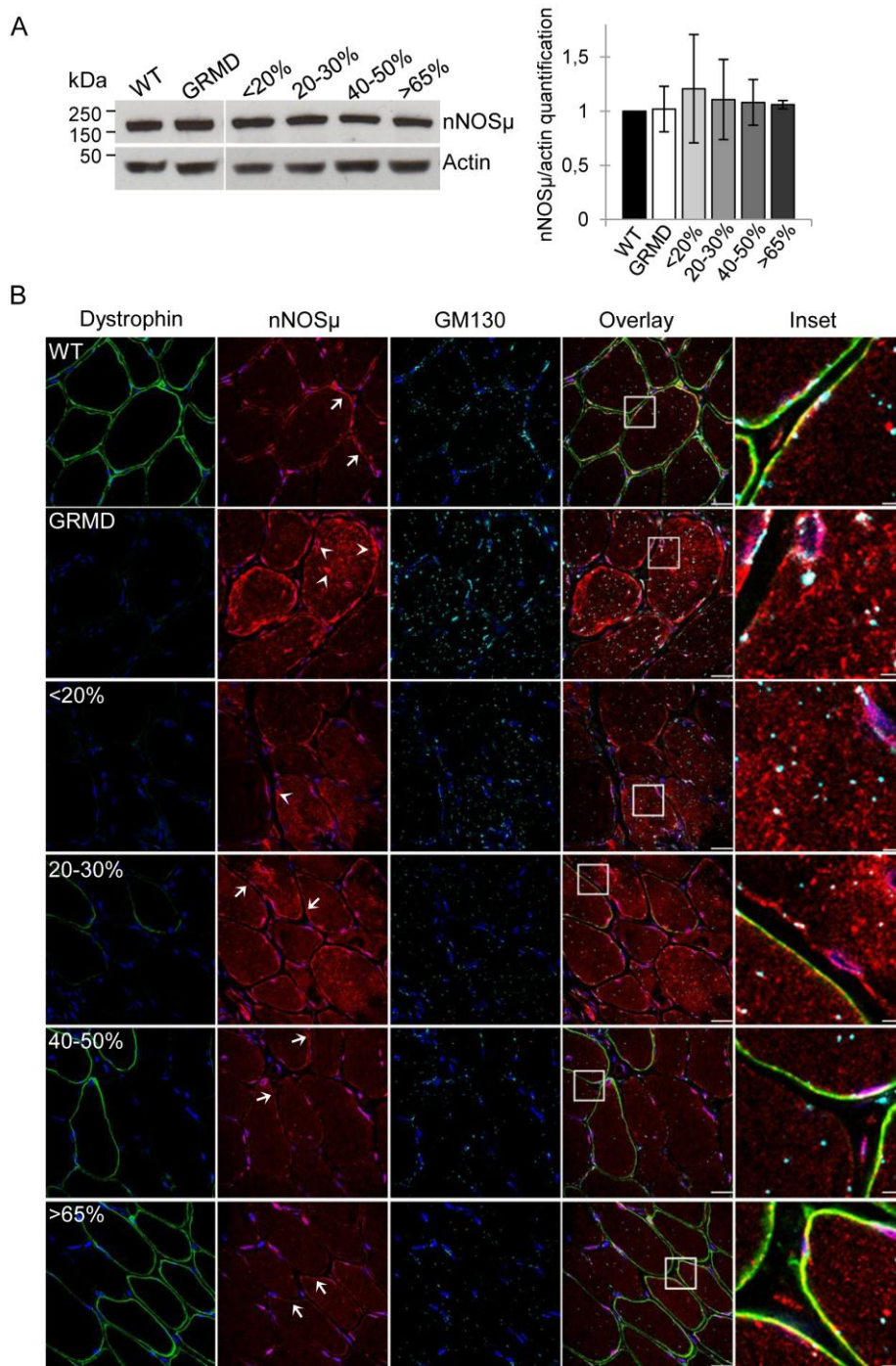
Figure 1: Restoration of dystrophin is associated with improvement of histopathophysiological features in canine muscle sections

(A) Representative immunolabeling of dystrophin on transverse cryosections of wild-type muscle (WT), untreated muscle from C2 (GRMD) and treated muscles from D13 expressing <20%, 20-30%, 40-50% or >65% of dystrophin-positive fibers. Nuclei were labeled with DAPI (blue). Scale bars: 200 μ m.

(B) Representative immunolabeling of dystrophin on longitudinal cryosections of treated muscles from D8 expressing 20-30% or >65% of dystrophin-positive fibers. Nuclei were labeled with DAPI (blue). Scale bars: 200 μ m.

(C) Representative hematoxylin and eosin staining on transverse cryosections of muscle samples from WT, untreated C2 (GRMD) and treated D13 expressing <20%, 20-30%, 40-50% or >65% of dystrophin-positive fibers. Scale bars: 100 μ m. Insets correspond to boxed regions, scale bars: 50 μ m. Arrowheads indicate centralized nuclei whereas arrows show endomysial fibrosis and adiposis.

Figure 2

**Figure 2: Restoration of dystrophin in 40% of fibers is needed to decrease the cytosolic nNOSμ**

(A) Representative western blot analysis of nNOSμ and actin on total protein extracts of muscle samples from WT, untreated C1 (GRMD) and treated D8 expressing <20%, 20-30%, 40-50% or >65%

of dystrophin-positive fibers. Quantification of nNOS μ expression normalized to actin signal. Results are expressed as mean \pm s.e.m., n=3 independent experiments.

(B) Representative immunolabeling of dystrophin, nNOS μ and GM130 on transverse cryosections of muscle samples from WT, untreated C1 (GRMD) and treated D13 expressing <20%, 20-30%, 40-50% or >65% of dystrophin-positive fibers. Nuclei were labeled with DAPI (blue). Arrowheads indicate cytosolic and sub-sarcolemmal aggregates of nNOS μ whereas arrows show the sarcolemmal location of nNOS μ . Scale bars: 20 μ m. Insets correspond to boxed regions, scale bars: 4 μ m.

Figure 3

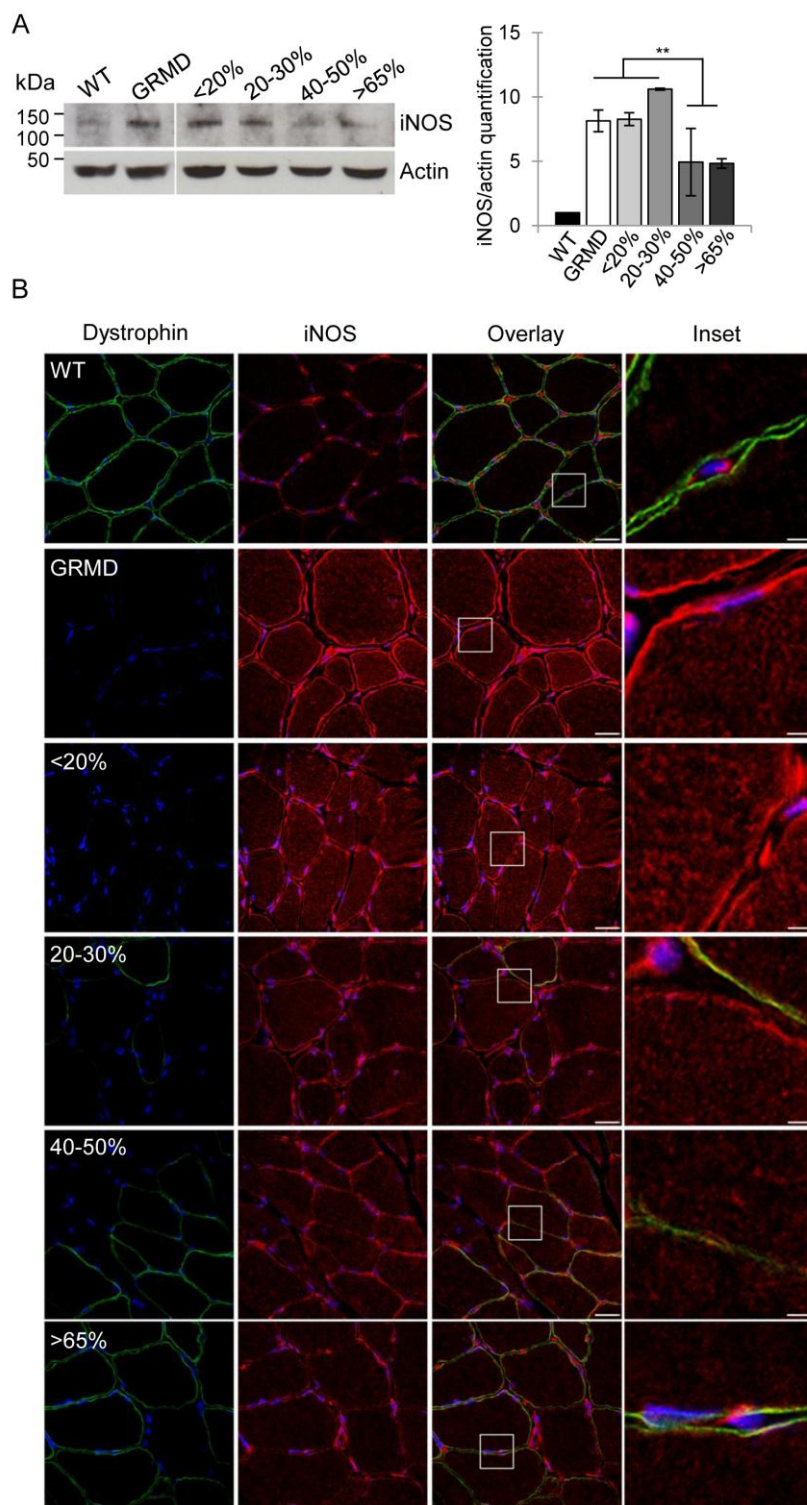


Figure 3: Restoration of dystrophin in 40% of fibers is needed for the reinstatement of iNOS expression

(A) Representative western blot analysis of iNOS and actin on total protein extracts of muscle samples from WT, untreated C1 (GRMD) and treated D8 expressing <20%, 20-30%, 40-50% or >65% of

dystrophin-positive fibers. Quantification of iNOS expression normalized to actin signal. Results are expressed as mean \pm s.e.m., ** $p < 0.01$, $n = 3$ independent experiments.

(B) Representative immunolabeling on transverse cryosections of muscle samples from WT, untreated C1 (GRMD) and treated D13 expressing <20%, 20-30%, 40-50% or >65% of dystrophin-positive fibers stained with anti-dystrophin and anti-iNOS. Nuclei were labeled with DAPI (blue). Scale bars: 20 μ m. Insets correspond to boxed regions, scale bars: 4 μ m.

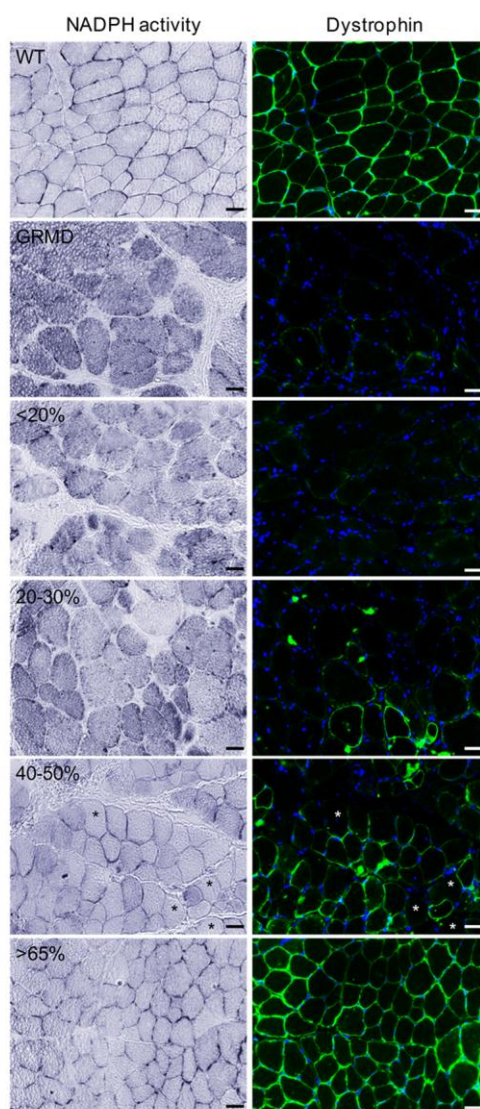


Figure 4: Restoration of dystrophin in 40% of fibers leads to a major reduction of cytosolic NO level

NADPH diaphorase activity staining visualized by the colorless soluble tetrazolium salt (blue staining) and dystrophin labeling on transverse cryosections of muscle samples from WT, untreated C2 (GRMD) and treated D13 expressing <20%, 20-30%, 40-50% or >65% of dystrophin-positive fibers. Asterisks indicate dystrophin-negative fibers displaying a major reduction of cytosolic NO production. Scale bars: 25 μ m.

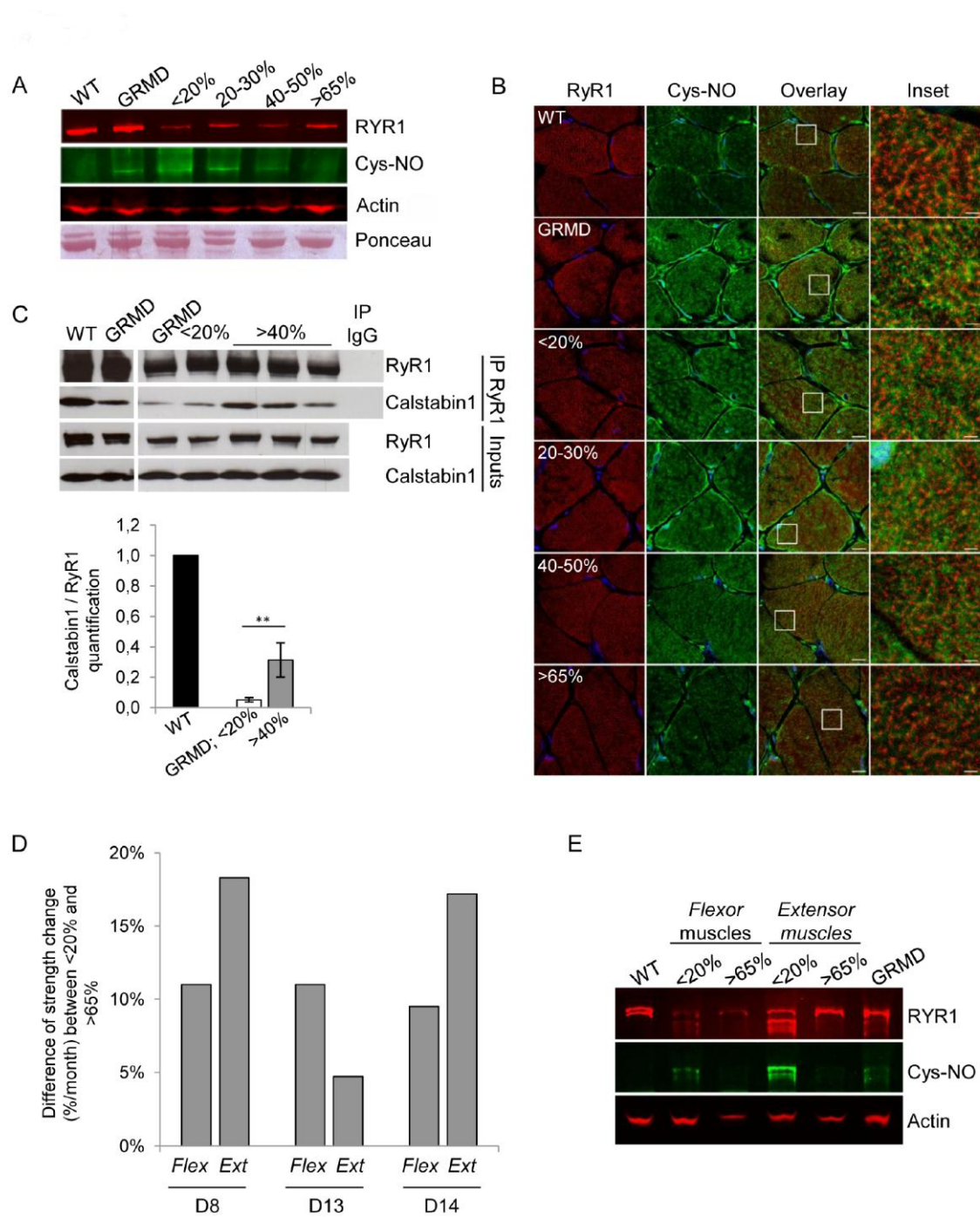


Figure 5: Restoration of dystrophin in 40% of fibers is needed to stabilize RyR1/calstabin1 complex

(A) Representative multiplex western blot assessing RyR1 hypernitrosylation on total protein extracts of muscles from WT, untreated C1 (GRMD) and treated D13 expressing <20%, 20-30%, 40-50% or >65% of dystrophin-positive fibers. RyR1 (red) and Cys-NO (green) labeling were detected simultaneously by separate fluorescent channel. Actin staining and Ponceau red staining illustrated the loading proteins of each muscle extract.

(B) Representative immunolabeling of RyR1 and Cys-NO on transverse cryosections of muscle samples from WT, untreated C2 (GRMD) and treated D13 expressing <20%, 20-30%, 40-50% or >65% of dystrophin-positive fibers. Nuclei were labeled with DAPI (blue). Scale bars: 10 μ m. Insets correspond to boxed regions, scale bars: 4 μ m. Representative western blot with RyR1 and calstabin1 antibodies of RyR1 immunoprecipitation (IP RyR1) in muscle samples from WT, untreated C1 and C2 (GRMD) and treated D14 expressing <20% or >40% of dystrophin-positive fibers. The total input allowed controlling the RyR1 and calstabin1 expression in each muscle extracts before IP. IgG was used as negative control.

(C) Quantification of western blot ($\text{IP}_{\text{Calstabin1}}/\text{inputs}_{\text{Calstabin1}}$) / ($\text{IP}_{\text{RyR1}}/\text{inputs}_{\text{RyR1}}$). Results are expressed as mean \pm s.e.m., **P<0.01, n=4 independent experiments.

(D) Difference of strength change per month (%/month) between *flexor* muscles or *extensor* muscles expressing <20% of dystrophin-positive fibers, and *flexor* muscles or *extensor* muscles expressing >65% of dystrophin-positive fibers, for D8, D13 and D14 dogs.

(E) Representative multiplex western blot assessing RyR1 hypernitrosylation on total protein extracts of muscle samples from WT, untreated C1 (GRMD), *flexor* muscle from D8 with <20% of dystrophin-positive fibers or with >65% of dystrophin-positive fibers and *extensor* muscle from D14 with <20% of dystrophin-positive fibers or with >65% of dystrophin-positive fibers. RyR1 (red) and Cys-NO (green) labeling were detected simultaneously by separate fluorescent channel and normalized to actin expression. n=3 independent experiments.

Table S1: Characteristics of the different muscle samples analyzed in this study

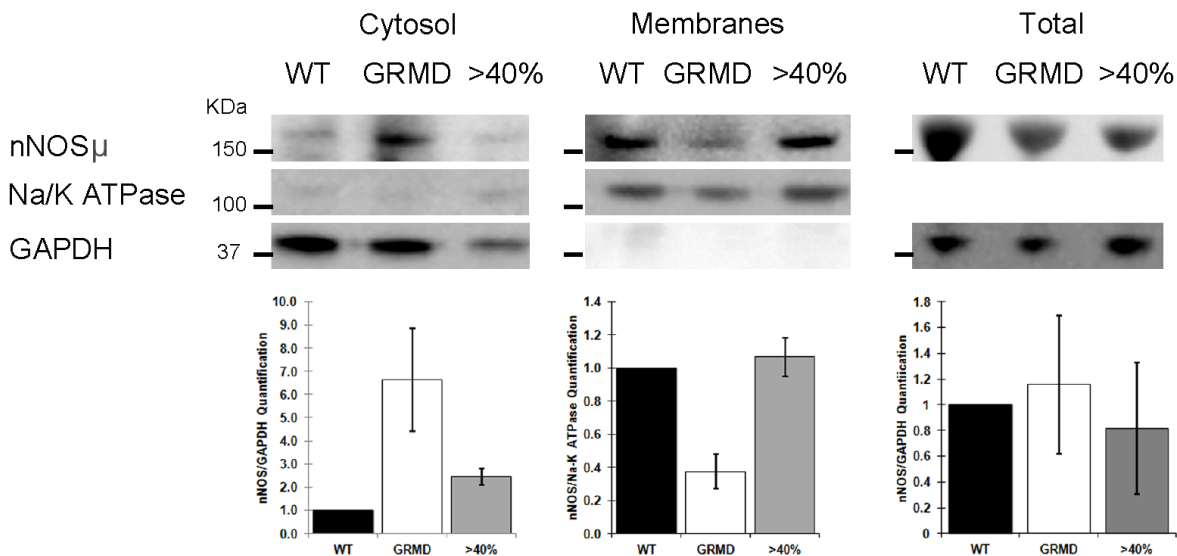


Figure S2: Abnormal intracellular location of nNOSμ is recovered at the sarcolemma of treated GRMD muscle fibers. Top: Representative western blot of nNOSμ on membrane and cytosolic fractions isolated from WT, untreated GRMD (dog C1) and treated muscle (dog D13) expressing >40% of dystrophin positive fibers, n=3. Western blots of Na/K ATPase and GAPDH typified the sarcolemmal or the cytosolic fractions respectively. Bottom: Signal quantification performed using Quantity one software and expressed by the ratio of the values obtained for nNOSμ/GAPDH and nNOSμ/Na-K ATPase for cytosol and membranes fraction respectively.

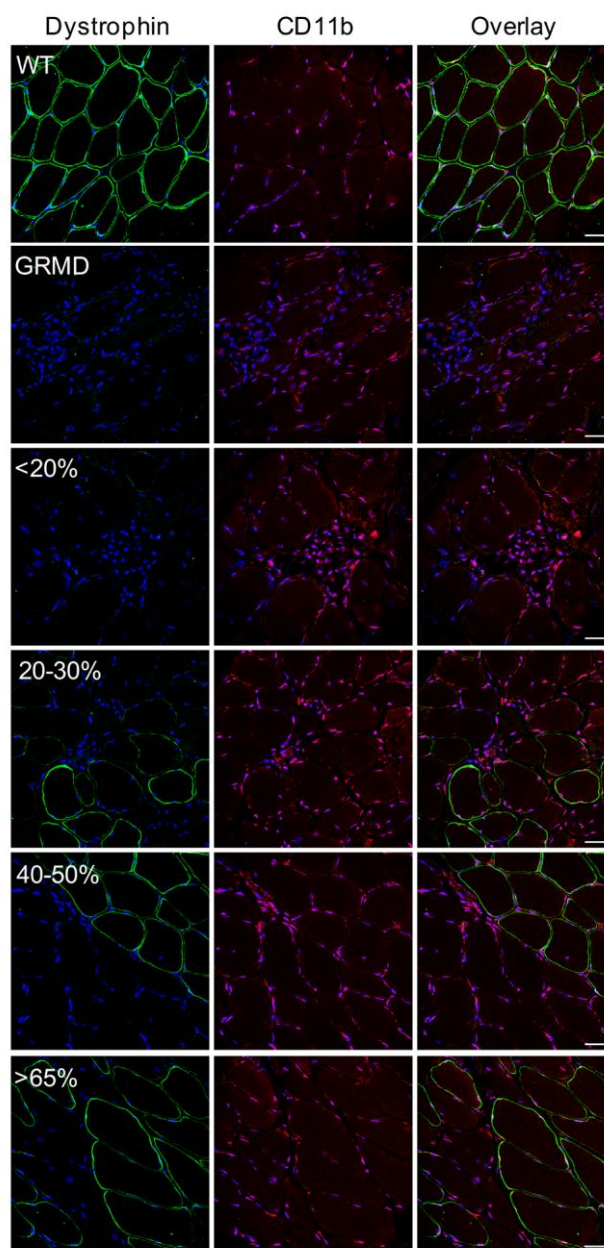


Figure S3: Decrease of inflammatory response by dystrophin expression

Representative immunolabeling of dystrophin and CD11b on transverse cryosections of muscle samples from WT, untreated C1 (GRMD) and treated D13 with <20%, 20-30%, 40-50% or >65% of dystrophin-positive fibers. Nuclei were labeled with DAPI (blue). Scale bars: 20 μ m.

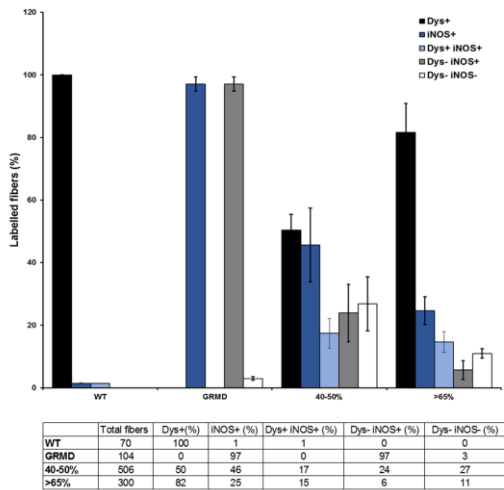


Figure S4: Quantification of the reinstatement of iNOS expression in dystrophin-restored muscles:

Top: Histogram of iNOS and dystrophin distribution in fibers from healthy (WT), untreated GRMD (dog C1) and D8, D13 and D14 muscles expressing either 40-50% or >65% of dystrophin-positive fibers. Bottom: Table of the analyzed samples used for the histogram.

Table S1: Characteristics of the different muscle samples analyzed in this study

Group	Dog	Type of injection	Volume % limb	Flow rate (mL/min)	% Dys+ fibers	Analysed muscles
Wild-type	WT	/	/	/	100%	Superficial flexor of fingers
Untreated GRMD	C1	Ringer-Lactate	40	19	<0,5%	Biceps
						Extensor carpi radialis
	C2	20	10	Deltoid		
Treated GRMD	D8	rAAV8-U7-E6/E8 5E+13 vg/kg	40	13	<20%	Flexor carpi radialis non injected
						Flexor carpi ulnaris non injected
						Extensor carpi radialis non injected
					20-30%	Biceps injected
					40-50%	Flexor digitorum profundus injected
					>65%	Extensor digitorum communis injected
						Flexor carpi ulnaris injected
						Extensor carpi radialis injected
	D13		20	10	<20%	Biceps injected
						Flexor carpi radialis non injected
						Flexor carpi ulnaris non injected
						Extensor carpi radialis non injected
					20-30%	Supra-thorn-bush injected
					40-50%	Abductor injected
					>65%	Extensor digitorum communis injected
						Flexor carpi ulnaris injected
						Extensor carpi radialis injected
	D14				<20%	Supraspinatus non injected
						Flexor carpi ulnaris non injected
						Extensor carpi radialis non injected
					20-30%	Supra-thorn-bush injected
					40-50%	Deltoid injected
					>65%	Ulnaris lateralis injected
						Flexor carpi ulnaris injected
						Extensor carpi radialis injected

